A Novel Ultra-Broadband Low-Loss Bond-Wire Interconnect Design Concept Applied to a 2 GHz to 135 GHz Substrate-to-Substrate Interface

Tim Pfahler[#1], Andre Scheder[#], Anna Bridier[*], Jan Schür[#], Martin Vossiek[#]
[#]Institute of Microwaves and Photonics, Friedrich-Alexander-Universität Erlangen-Nürnberg, Germany
[*]Rohde und Schwarz GmbH, Germany
[1]tim.m.pfahler@fau.de

***Abstract*— This work presents a design concept for ultra-broadband bond-wire interconnects between two alumina substrates from 2 GHz up to 135 GHz. Due to the rethinking of the substrate assembly and optimization of the CPW bond-wire transmission line interface, the currently existing limitations in terms of a narrowband matching bandwidth and high insertion loss of state-of-the-art interconnects can be eliminated. The resulting key advantage of the proposed design is the ultra-broadband characteristic that exhibits lowest impedance discontinuity and thus realizing an excellent matching bandwidth of more than 130 GHz. The measured return loss is higher than 25 dB with an insertion loss of less than 1.6 dB over the entire frequency band. The paper highlights both, the electric considerations as signal routing and the assembly part for achieving a robust, reproducible and fully mmW-transparent interconnect even beyond 100 GHz. Due to the broadband performance and the high agreement of simulation and measurement results the proposed interconnect and the underlying design and assembly considerations set a new benchmark for interconnect design. Moreover, this approach can be used for signal transitions in applications such as broadband communication systems, high-resolution radar sensing and measurement and test applications.**

***Keywords*— assembly, bond-wire, interconnect, monolithic microwave integrated circuits (MMIC), packaging, signal transition, measurement and test.**

I. Introduction and Motivation

The demand and the need for ultra-broadband systems for next generation communication links, high-resolution radar/imaging applications or broadband test and measurement devices is constantly increasing [1], [2], [3]. Especially in a heterogeneous system design (e.g. mixture/combinations of different technologies like MMIC, ceramics and printed circuit boards), the need for robust, suitable interconnects is tremendous, which are required to build entire systems and direct the wave propagation between different building block and modules [4]. Especially in the development of measurement and test instruments, it is important to reduce the reflections and losses of each interconnect to ensure the optimum measurement sensitivity due to the various and numerous interconnects as a whole. Different integration-techniques are currently available: flip-chip approaches, cavity-embedded MMICs or bond-wire interconnects. Nevertheless, the bottleneck in terms of bandwidth, insertion loss and matching behavior in the system integration is mostly the interconnect [3].

In our opinion, the limiting aspect of existing bond-wire interconnect designs are the substrate arrangements to each other, especially the gap between neighboring substrates and therefore the resulting bond-wire length, which leads to high impedance discontinuities. Those impedance discontinuities can be compensated by matching circuits even at frequencies above 100 GHz, but only in a very narrow frequency band (< 10 GHz) due to wavelength-dependent matching structures [5], [6]. In addition, existing approaches show significantly worse return loss (RL $\approx$ 10 dB) and, above all, much higher insertion losses (IL > 2-3 dB over the observed bandwidth) [1], [5], [6], [7]. Therefore, existing solutions are still far away from a so called "transparent interconnect" [3]. To overcome these limitations and to design broadband bond-wire interconnects with lowest insertion loss even above 100 GHz, the way how state-of-the-art interconnects are designed needs to be changed.

This is exactly where this approach comes in: We present an impedance-controlled bond-wire interconnect which achieves ultra-broadband signal transitions with high repeatability, automatable bond-wire assembly and robust against temperature expansions. This results in a minimal insertion loss (IL < 1.6 dB) due to distinguished return loss (RL > 25 dB) and assembly technology. This work therefore demonstrates the design procedure for excellent bond-wire performance even above 100 GHz and sets a new benchmark in interconnect design (see Table 1).

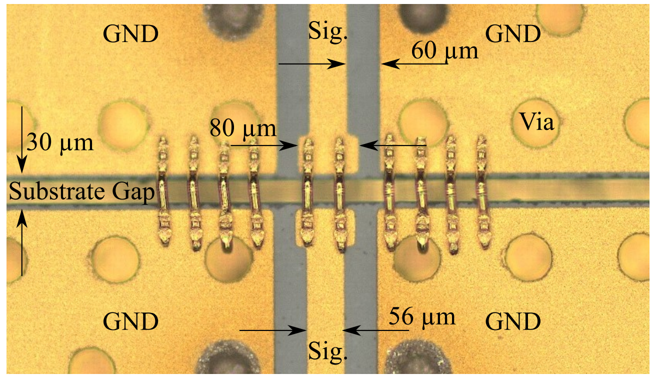

Fig. 1. Top view of proposed substrate assembly, bond-wire interface, substrate gap and dimensions of transmission line and bond-tail landing pads.

Table 1. Comparison of broadband interconnects. (* marks the de-embedded insertion loss of the bond-wire itself without transmission-line loss. ** back-to-back assembly)

Ref.	meas. match. bandwidth	meas. match. level	max. meas. insertion loss	interconnect technology
[1]	84 GHz	RL > 13 dB	IL < 3 dB	bond-wire
[3]	500 GHz	RL > 15 dB	IL < 1.8 dB	flip-chip**
[4]	100 GHz	RL > 12 dB	not known	flip-chip
[5]	10 GHz	RL > 10 dB	IL < 3 dB	bond-wire
[6]	100 GHz	RL > 7.5 dB	IL < 2.5 dB	bond-wire
[7]	220 GHz	RL > 8 dB	IL < 2.5 dB	quilt-package
This	**> 130 GHz**	**RL > 25 dB**	**IL < 1.6 dB** (IL* < 0.6 dB)	**bond-wire**

II. ASSEMBLY AND INTERCONNECT DESIGN CONSIDERATIONS

A. SUBSTRAT SELECTION AND ASSEMBLY

For the signal transmission a grounded coplanar waveguide (CPWG) is used and manufactured on an Alumina substrate of 4-mil thickness. Due to the chosen thickness parasitic modes can be suppressed up to the maximum frequency of interest within the substrate. In addition, the substrate height is similar to those of existing MMICs ($\approx 100\,\mu\text{m}$), resulting in a compact substrate-to-substrate or MMIC transition without the need for pedestals or cavities in the carrier. Therefore, the gap-width between two substrates or substrate-to-MMIC can be reduced significantly, which results in shorter bond length and less impedance mismatch (see Subsec. II-B). Due to the high substrate permittivity ($\varepsilon_\text{r} = 9.7$) compact waveguide structures can be designed. The $50\,\Omega$ CPWG waveguide was realized with a signal width of $56\,\mu\text{m}$ and a gap of $60\,\mu\text{m}$ (see Fig. 1). The transmission lines were made of gold (thickness of $4\,\mu\text{m}$) for minimal insertion loss and low surface roughness. The two substrates were applied to a carrier with conductive adhesive. Here, attention was paid that the adhesive does not rise in the substrate gap and disturbs or blocks the mmW-transition. The gap between the substrates is 30 μm. This is a compromise of several aspects: on the one hand, the gap must be large enough to allow thermal expansion of the individual substrates, on the other hand, the interconnect should be compact enough to allow signal transition with minimal impedance mismatch. The more compact the connection, the shorter the bond-wire, the less inductance has to be compensated for. Moreover, the arrangement of the substrates must be automatable to enable a practical interconnect for series production with simultaneous consideration of manufacturing and assembly tolerances. For positioning, the alignment marks on the carrier are scanned, the substrates are registered with a camera and placed on the carrier.

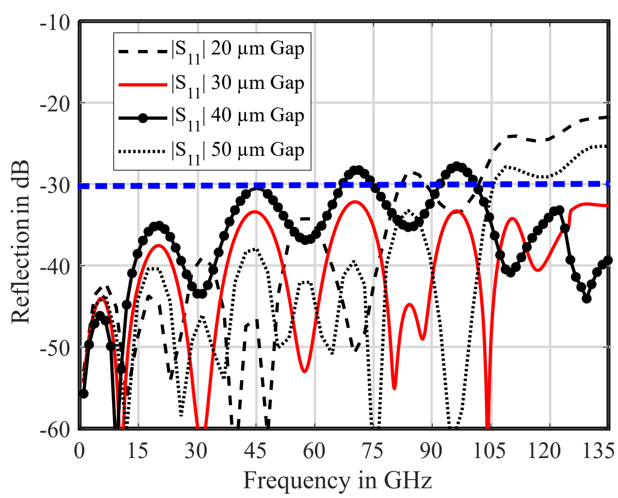

Fig. 2. Simulated reflection of the interconnect for different gaps between the substrates.

Cascading multiple bond-wire connected circuits or MMICs as a system can only provide optimum performance if the individual bond-wire interconnect is perfectly matched. The sufficient performance criterion in the simulation setup was a reflection level $|s_{11}|$ below $-30\,\text{dB}$. In Fig. 2 $|s_{11}|$ is plotted over frequency for different substrate gaps. The increase in reflection and therefore the decrease of performance is visible for wider gaps above $65\,\text{GHz}$ (blue threshold line in Fig. 2). This performance degradation must already be taken into account in the simulation stage in order to still have sufficient margins for the assembly; otherwise, the measured matching reflection level becomes significantly worse. The reflection level of the interconnect with a gap of $30\,\mu\text{m}$ (red trace) is constantly below $-30\,\text{dB}$, therefore an excellent choice for defining an mmW-transparent interconnect over the entire frequency band of interest with simultaneously enough mechanical margin for thermal expansion and assembly tolerances.

B. DESIGN OF BOND-WIRE INTERFACE

Two parallel bond-wires (diameter of $17.5\,\mu\text{m}$) were used to connect the signal traces of both substrates to reduce the total inductance (see Fig. 1). The lateral separation of the signal bonds is $45\,\mu\text{m}$, representing a compromise between performance and automated assembly of the bonds.

The landing pads ($80\,\mu\text{m}$ x $60\,\mu\text{m}$) for the signal bonds fulfill two critical aspects at once: First, they compensate for the

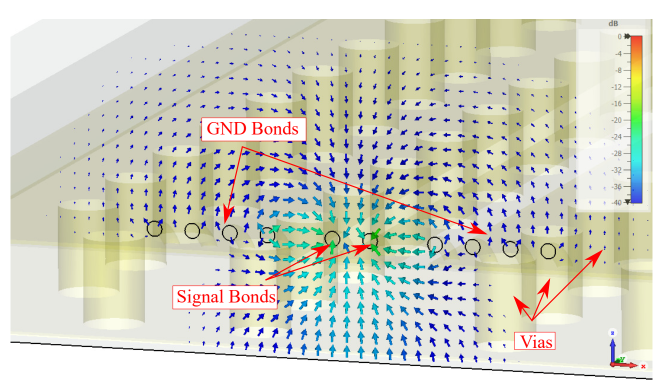

Fig. 3. Electric field distribution at 130 GHz within the CPW bond-wire transition at the center of the substrate gap (cutting plane).

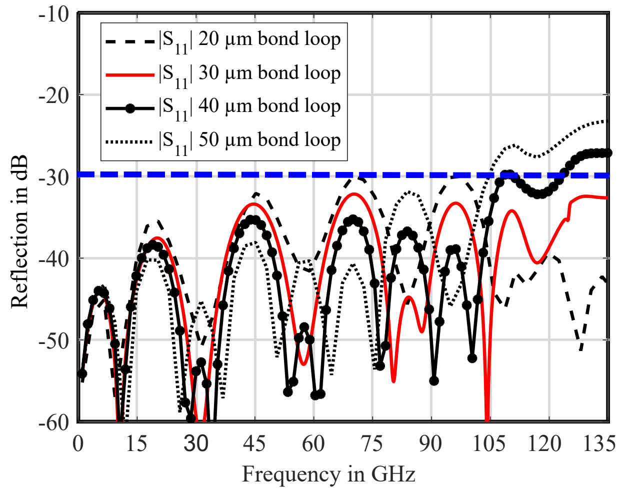

Fig. 4. Simulated reflection of the bond-wire interconnect for different bond loops.

inductive bond wires through their capacitive behavior, and second, the landing pad is large enough that the entire bond tail is placed on the pad. Otherwise protruding parts of the tail will cause unspecific parasitic distortion and capacity, resulting in worse performance of the interconnect.

The main advantage of the CPWG waveguide compared to e.g. microstrip is the ground (GND) connection on top of the substrate. Therefore, also a solid GND connection of the transition was realized and optimized by four bond-wires on each side. This is illustrated in Fig. 3. The number and spacing of the GND bonds were chosen so that the electric field drops laterally to a value of less than $-40\,\text{dB}$ with respect to the electric field maximum, thus decaying to a level where it no longer has an impact on system performance. The inner ground bond was placed close to the gap of the CPWG for less interference of the EM field distribution. The electric field distribution within the gap matches very well with the CPWG field distribution on the substrate (cutting plane at 130 GHz, see Fig. 3). Due to the great conformity of the field distribution, the impedance mismatch within the transition can be minimized. In addition, the bond-wire interface can be modeled as a CPW transmission line interface with an impedance close to $50\,\Omega$, resulting in lowest impedance discontinuity and thus ideal matching behavior. The whole setup was designed and optimized in the frequency domain within the 3D-EM simulation tool CST [8].

An important optimization step, a key component for the overall interconnect performance, was the decision on the bond-wire loop. Similar to the selection of a proper substrate gap, several aspects had to be taken into account when choosing the optimal loop. On the one hand, the loop should be as low as possible, resulting in short overall bond length and thus lower inductance. On the other hand, a minimal loop is required to withstand thermal expansion of the substrates, assembly tolerances or minimal height misalignment. Otherwise, the bond-wire will crack during expansion. The effect and impact of different bond loops is illustrated in Fig. 4. At frequencies above $100\,\text{GHz}$, the performance decreases with increasing bond loop, and therefore bond inductance. The assembly with $20\,\mu\text{m}$ bond height has too little loop and thus mechanical strength/margin to withstand thermal expansion. The inductance in variants with $40\,\mu\text{m}$ or $50\,\mu\text{m}$ bond heights is too large due to the resulting length, which leads to poorer performance in the simulation, and thus insufficient scope for an assembly. The optimum is found at a bond loop height of $30\,\mu\text{m}$, a combination of electric performance and mechanical stability and durability. The reflection coefficient is constantly below $|s_{11}| < 30\,\text{dB}$ within the simulation and thus represents an ideal candidate for the assembly. The assembled bond-wire transition (Fig. 1) has a measured bond loop height of $32\,\mu\text{m}$, therefore is in excellent agreement with the target value.

III. Measurement Setup

To enable such frequency continuous ultra-broadband characterization of the proposed interconnect, the measurement range was divided into two parts: first, the sample was measured with coaxial waveguide probes from 2 - $110\,\text{GHz}$ with a PNA-X vector analyzer and waveguide modules from Agilent Technologies. In a second step, the characterization was performed with the identical vector analyzer and frequency extenders (R&S ZVA-Z170) from 110 - $135\,\text{GHz}$. In this case, the circuit was contacted with Infinity GSG probes (WR 6.5). In both scenarios, the measurement setup was calibrated with a custom-made TRL calibration kit with different line length realized on the same substrate. Therefore, the reference plane of the ultra-broadband characterization is directly on the CPWG-transmission line.

IV. Measuremental Characterization

The comparison of the measured and simulated reflection coefficient of the proposed interconnect is shown in Fig. 5. The results correspond perfectly over the entire frequency band. Special attention should be paid on the reflection level. The measured value is constantly below $-25\,\text{dB}$, confirming an

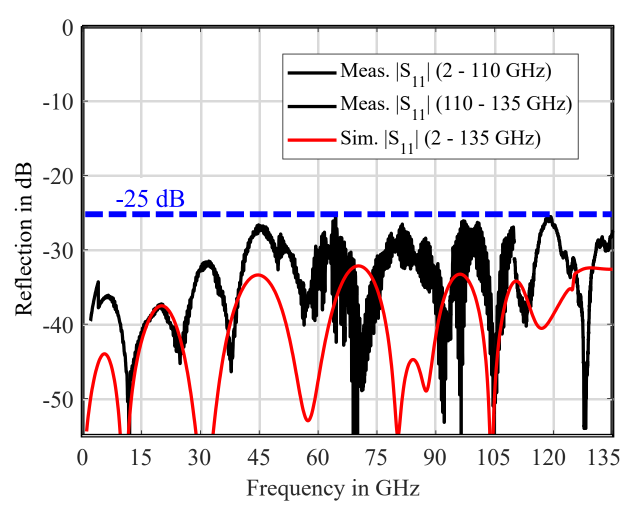

Fig. 5. Simulated and measured reflection of the bond-wire interconnect.

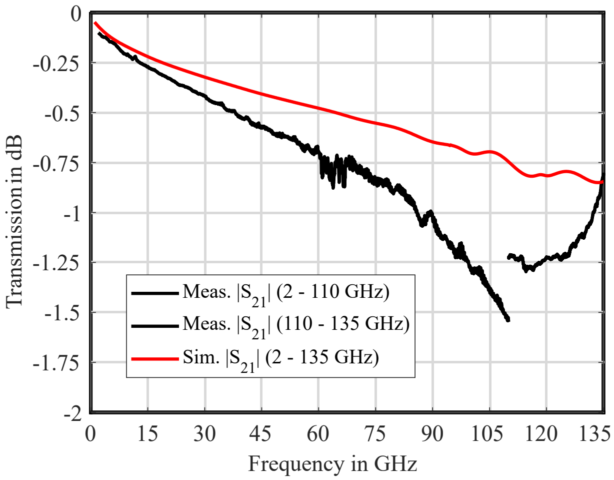

Fig. 6. Simulated and measured transmission of the bond-wire interconnect.

ultra-broadband mmW-transparent interconnect. This matching behavior is not achieved by losses in the substrate or conductor, but by the excellent mmW-performance, its bond-wire interface design and the assembly of bond-wires and substrates. This can be proven by the inspection of the transmission coefficient of the proposed interconnect in Fig. 6. The measured insertion loss is below $1.6\,\mathrm{dB}$ over the entire frequency band of interest. With the help of a multiline method using CPWG-transmission lines of different lengths, it was possible to determine the attenuation per CPWG-line length. This made it possible to decouple the losses of the CPWG-feedline ($2.3\,\mathrm{mm}$ each on both sides of the interconnect) so that the resulting insertion loss of the bond-wire itself can be de-embedded to less than $0.6\,\mathrm{dB}$ over the entire frequency band (see Table 1). The high correspondence between measurement and simulation results indicates a suitable modeling of the bond-wire geometries within the simulation setup, a valid interconnect design and its functionality. Furthermore, the difference $\Delta|s_{21}|$ in the measured insertion of less than $0.3\,\mathrm{dB}$ at the transition frequency ($110\,\mathrm{GHz}$) of the two measurement ranges clarifies the calibration procedure and a valid measurement setup for such ultra-broadband mmW-characterizations.

V. Conclusion

This work demonstrates an ultra-broadband bond-wire signal transition with measured minimal reflection ($|s_{11}| < -25\,\mathrm{dB}$) and lowest insertion loss (IL < $1.6\,\mathrm{dB}$) over the entire frequency band from 2 - $135\,\mathrm{GHz}$. The rethinking and redesigning of the substrate arrangement and the optimized bond-wire interface eliminate the current limitations in bandwidth and insertion loss performance of state-of-the-art approaches. The work highlights the design considerations for automated substrate and bond-wire assembly and the necessary optimization steps for the development of a reproducible, robust impedance-controlled signal transition between substrate-to-substrate or MMIC. The key advantage of this compact interconnect design is that the dimension are smaller than $\lambda_0/10$, therefore not wavelength-dependent. Thus, an almost bandwidth-independent matching behavior is achieved (> $130\,\mathrm{GHz}$). Especially the low insertion loss above $100\,\mathrm{GHz}$ (IL < $0.6\,\mathrm{dB}$ (de-embedded bond-wire IL)) due to the optimized bond-wire interface and the substrate assembly is a new benchmark for interconnect design. This work can be used as a reference design for achieving excellent bond-wire interconnect performance for building heterogeneous communication, sensing or measurement and test applications with system bandwidth above $100\,\mathrm{GHz}$.

Acknowledgment

The Bavarian State Ministry of Economic Affairs, Regional Development and Energy supported this work through the joint research project MIDAS (Grant No. DIE0112/02). The authors would like to thank Rohde & Schwarz, especially Frank Eberhardt, Gerhard Duile and Ronny Raupach for the precise manufacture of the specimens and the excellent assembly technique.

References

[1] C.-H. Li, C.-L. Ko, C.-N. Kuo, M.-C. Kuo, and D.-C. Chang, "A low-cost dc-to-84-ghz broadband bondwire interconnect for sop heterogeneous system integration," *IEEE Transactions on Microwave Theory and Techniques*, vol. 61, no. 12, pp. 4345–4352, 2013.

[2] J. Hasch, E. Topak, R. Schnabel, T. Zwick, R. Weigel, and C. Waldschmidt, "Millimeter-wave technology for automotive radar sensors in the 77 ghz frequency band," *IEEE Transactions on Microwave Theory and Techniques*, vol. 60, no. 3, pp. 845–860, 2012.

[3] W. Heinrich, M. Hossain, S. Sinha, F.-J. Schmückle, R. Doerner, V. Krozer, and N. Weimann, "Connecting chips with more than 100 ghz bandwidth," *IEEE Journal of Microwaves*, vol. 1, no. 1, pp. 364–373, 2021.

[4] W. Heinrich, "The flip-chip approach for millimeter wave packaging," *IEEE Microwave Magazine*, vol. 6, no. 3, pp. 36–45, 2005.

[5] S. Beer, H. Gulan, M. Pauli, C. Rusch, G. Kunkel, and T. Zwick, "122-ghz chip-to-antenna wire bond interconnect with high repeatability," in *2012 IEEE/MTT-S International Microwave Symposium Digest*, 2012, pp. 1–3.

[6] S. Fikar, R. Bogenberger, and A. L. Scholtz, "A 100ghz bandwidth matched chip to pcb transition using bond wires for broadband matching," in *2008 12th IEEE Workshop on Signal Propagation on Interconnects*, 2008, pp. 1–4.

[7] P. Fay, D. Kopp, T. Lu, D. Neal, G. H. Bernstein, and J. M. Kulick, "Ultrawide bandwidth chip-to-chip interconnects for iii-v mmics," *IEEE Microwave and Wireless Components Letters*, vol. 24, no. 1, pp. 29–31, 2014.

[8] "Cst studio suite," 2021. [Online]. Available: http:// www.3ds.com